Since January 2020 Elsevier has created a COVID-19 resource centre with free information in English and Mandarin on the novel coronavirus COVID-19. The COVID-19 resource centre is hosted on Elsevier Connect, the company's public news and information website.

Available online at www.sciencedirect.com
SCIENCE DIRECT®
Experimental Neurology 187 (2004) 254–265
Experimental Neurology
www.elsevier.com/locate/yexnr

Remyelination, axonal sparing, and locomotor recovery following transplantation of glial-committed progenitor cells into the MHV model of multiple sclerosis

Minodora O. Totoiu,[a] Gabriel I. Nistor,[a] Thomas E. Lane,[b] and Hans S. Keirstead[a,*]

[a] *Reeve-Irvine Research Center, Department of Anatomy and Neurobiology, College of Medicine, University of California at Irvine, 2111 Gillespie Neuroscience Research Facility, Irvine, CA 92697-4292, USA*
[b] *Department of Molecular Biology and Biochemistry, University of California at Irvine, 2238 McGaugh Hall, Irvine, CA, 92697-3900, USA*

Received 15 August 2003; revised 25 November 2003; accepted 22 January 2004

Available online 21 March 2004

Abstract

The behavior and myelinogenic properties of glial cells have been well documented following transplantation into regions of focal experimental demyelination in animal models. However, the ability of glial cell preparations to remyelinate in such models does not necessarily indicate that their transplantation into demyelinated lesions in clinical disease will be successful. One of the precluding factors in this regard is a greater understanding of the environmental conditions that will support transplant-mediated remyelination. In this study, we determined whether the complex and reactive CNS environment of the mouse hepatitis virus (MHV) model of multiple sclerosis (MS) could support transplant-mediated remyelination. Striatal neural precursors derived from postnatal day 1 mice were committed to a glial cell lineage and labeled. Immunohistochemical staining indicated that this population generated >93% glial cells following differentiation in vitro. Transplantation of glial-committed progenitor cells into the T8 spinal cord of MHV-infected mice demonstrating complete hindlimb paralysis resulted in migration of cells up to 12 mm from the implantation site and remyelination of up to 67% of axons. Transplanted-remyelinated animals contained approximately 2× the number of axons within sampled regions of the ventral and lateral columns as compared to non-transplanted animals, suggesting that remyelination is associated with axonal sparing. Furthermore, transplantation resulted in behavioral improvement. This study demonstrates for the first time that transplant-mediated remyelination is possible in the pathogenic environment of the MHV demyelination model and that it is associated with locomotor improvement.

Keywords: Stem cell; Oligodendrocyte; Remyelination; MHV; Multiple sclerosis; Glia; Demyelination

Introduction

Remyelination is a successful regenerative event within the adult central nervous system (CNS), as it can restore saltatory conduction (Smith et al., 1979) and facilitate functional recovery (Jeffery and Blakemore, 1997). Remyelination has been demonstrated in a variety of experimental demyelination/mutant models (Blakemore, 1973, 1974, 1975, 1982; Duncan et al., 1988; Gumpel et al., 1989; Herndon et al., 1977; Jeffery and Blakemore, 1995, 1997; Jeffery et al., 1999; Keirstead and Blakemore, 1999; Moore et al., 1985; Rodriguez et al., 1987; Sasaki and Ide, 1989; Yajima and Suzuki, 1979) and occurs spontaneously in naturally occurring demyelinating diseases such as MS (Prineas et al., 1993a). However, remyelination failure is more prevalent than its success when considering the spectrum of pathologies that affect the CNS. Although remyelination is usually successful in most animal models, it is often incomplete in the Theiler's model of demyelination (Murray et al., 2001). Furthermore, remyelination is less efficient in old animals than in young animals (Shields et al., 1999). The failure of remyelination is illustrated within foci of chronic demyelination within the later stages of MS (Prineas et al., 1993b). Chronic MS lesions are characterized by oligodendrocyte loss (Ozawa et al., 1994), with remyelination limited to the borders of inactive plaques (Suzuki et al., 1969).

* Corresponding author. Fax: +1-949-824-9272.
E-mail address: hansk@uci.edu (H.S. Keirstead).
URL: http://www.reeve.uci.edu/.

0014-4886/$ - see front matter © 2004 Elsevier Inc. All rights reserved.
doi:10.1016/j.expneurol.2004.01.028

Repairing persistent demyelination may ameliorate clinical deterioration. In addition to restoring normal impulse conduction (Utzschneider et al., 1994), remyelination may decrease axonal degeneration/transection. This is suggested by the demonstration that chronically demyelinated axons are vulnerable to degeneration/transection and that axonal loss in the later stages MS contributes to clinical deterioration (Bjartmar et al., 1999; De Stefano et al., 1998; Trapp et al., 1998). These findings underscore the importance of developing therapeutic strategies to enhance remyelination. One approach is to activate or enhance the response of endogenous mechanisms for repair, as has been demonstrated following growth factor administration in the experimental autoimmune encephalomyelitis (EAE) demyelination model (Yao et al., 1995), or passive transfer of antiserum (Rodriguez et al., 1987) or purified immunoglobulin (Rodriguez and Lennon, 1990) from mice immunized with spinal cord homogenate into the Theiler's demyelination model (Miller and Rodriguez, 1995). An alternative approach to remyelinating areas of demyelination is the transplantation of remyelination-competent cells.

Stem cells and neural precursors represent attractive sources for the generation of remyelination-competent cells, as they can be readily amplified and differentiated to the oligodendrocyte lineage (Ben-Hur et al., 1998; Brustle et al., 1999). Stem cell-derived glial precursors have been shown to myelinate following transplantation into the myelin-deficient rat (Brustle et al., 1999), and neural precursor-derived glial-committed progenitors (Ben-Hur et al., 1998; Keirstead et al., 1999) have been shown to myelinate following transplantation into regions of acute experimental demyelination (Keirstead et al., 1999). More recently, intracerebroventricular or intrathecal implantation of neural precursors into the EAE demyelination model resulted in migration of transplanted cells into white matter and their differentiation to astrocytes and oligodendrocytes, although no assessment of their ability to myelinate was performed (Ben-Hur et al., 2003). To determine whether transplantation represents a viable strategy for treating demyelination, it is necessary to better understand the range of environmental conditions that support transplantation-mediated remyelination.

In this study, we investigated the ability of the complex and reactive disease state of the chronic demyelinating MHV model of MS to support transplant-mediated remyelination. Intracerebral injection of the J2.2v-1 strain of MHV results in acute encephalomyelitis with demyelination, followed 10–12 days later by an immune-mediated demyelinating encephalomyelitis with hindlimb paralysis and progressive CNS destruction, including the initiation of new demyelination foci probably for the life of the mouse (Fleming et al., 1987; Haring and Perlman, 2001; Lane et al., 1998; Stohlman and Hinton, 2001; Stohlman et al., 2002). This model provides an environment of ongoing demyelinating pathogenesis, and is thus distinct from gliotoxin lesions. Intraspinal transplantation of glial-committed progenitors into the MHV model of MS resulted in extensive migration of transplanted cells, robust remyelination, axonal sparing, and behavioral improvement. These results show that transplant-mediated remyelination is possible following intraspinal transplantation into an environment of ongoing pathogenesis resembling MS.

Material and methods

Cell culture

Striata from 4 postnatal day 1 C57BL/6 mice were dissected, triturated, and maintained as previously described (Ben-Hur et al., 1998). Trypan blue was used to determine cell viability. Cells were grown for 5 days as floating clusters in 6-well low-adherent plastic dishes (Corning Life Sciences Acton, MA) at an initial density of 2×10^6 cells/5 ml of DMEM:F12, B27 supplement (Gibco-Invitrogen, Carlsbad, CA) with insulin, sodium selenite, transferrin, putrescin, progesterone, T3, detailed in Ben-Hur et al. (1998), and 0.02 μg/ml epidermal growth factor (EGF; Sigma-Aldrich, St. Louis, MO). On day 2, culture supernatant containing the floating clusters was removed and centrifuged at 400× *g* for 5 min. Clusters were then resuspended in fresh media and added to new culture dishes. On day 3, 0.02 μg/ml EGF was added to the culture dishes. On day 4, clusters were washed, resuspended in fresh media, and added to new culture dishes. On day 5, clusters were incubated with 10 mM BrdU (Sigma-Aldrich) in the culture medium overnight. One culture dish was not labeled with BrdU to compare viability and differentiation in the presence and absence of BrdU. On day 6, cultures were prepared for transplantation. Clusters were dissociated with 0.05% Trypsin-EDTA (Invitrogen Canada Inc., Burlington, ON) for 5 min, triturated, centrifuged for 5 min at 400 × *g*, resuspended three times in calcium- and magnesium-free DMEM (Gibco-Invitrogen), and concentrated to a final density of 12×10^4 cells/μl in the same media. The cell preparation was kept on ice for a maximum of 1 h before transplantation. On the day of transplantation, some cells were prepared for immunocytochemistry. Clusters were centrifuged for 5 min at 400 × *g* and resuspended three times in fresh media without EGF, and were plated on 10 mg/ml poly-L-lysine (Sigma-Aldrich) and 15 μg/ml laminin (Sigma-Aldrich) coated four chamber, imaging slides (Nalgene-Nunc International, Rochester, NY).

Immunocytochemistry

To assess differentiation potential, cells were grown on imaging slides on adherent substrate for 7 days, then fixed in 4% paraformaldehyde (Fisher Scientific, Pittsburgh, PA) in PBS for 10 min and immunocytochemical staining was

performed using standard protocols. Imaging chambers were blocked with 20% normal goat serum (NGS) (Chemicon, Temecula, CA) for 30 min at room temperature. Primary antibodies (polyclonal rabbit anti-GalC, Chemicon, 1:200 dilution in 4% NGS; monoclonal mouse anti-NeuN, Chemicon, 1:200 dilution in 10% NGS; polyclonal rabbit anti-GFAP, DAKO, Denmark, 1:200 dilution in 4% NGS; monoclonal mouse anti-CD 11 b, Serotec, UK, 1:200 dilution in 4% NGS; polyclonal rat anti-BrdU, Accurate Chemical and Scientific Corporation, Westbury, NY, 1:200 dilution in 4% NGS) were applied to imaging chambers overnight at 4°C. Imaging chambers were rinsed three times with PBS, incubated for 30 min in 4% NGS, and fluorescent-conjugated secondary antibodies (Alexa 488 or 594, goat anti-rabbit, goat anti-rat, or goat anti-mouse IgG H+L, 1:200 dilution in 4% NGS; Vector Laboratories, Burlingame, CA) was applied and incubated for 1 h at room temperature. Chambers were rinsed three times in PBS, and nuclear staining was conducted by exposing cultures to bis-benzimide (Hoechst 33258, Molecular Probes, Eugene, OR) for 10 min. Cell quantification was conducted using an Olympus AX-80 light microscope with a 20× objective. The percentage of immunopositive cells was determined by dividing the total number of immunopositive cells by the total number of Hoechst-positive cells in each imaging chamber, and averaging the results from three different imaging chambers per marker. A total of 1940 Hoechst-positive cells were counted for these analyses. Each 4-chamber imaging slide had one no-primary control chamber and three stained chambers for each of the markers mentioned above. Only immunopositive cells with clearly Hoechst-positive nucleus were counted.

MHV model

Age-matched, weight-matched (20–22 g) male C57BL/6 mice (H-2^b background; National Cancer Institute, Bethesda, MD; $n = 16$) were anesthetized by methoxyflurane inhalation (Pitman-Moore Inc., Washington Crossing, NJ). Mice received intracerebral injections of 500 plaque forming units of the neurotropic corona virus MHV strain J2.2v-1 (kindly provided by J. Fleming, University of Wisconsin, Madison, WI), suspended in 30 μl of sterile saline (Lane et al., 1998). Intracerebral injection of MHV results in a biphasic disease: acute encephalomyelitis with myelin loss, followed 10–12 days later by an immune-mediated demyelinating encephalomyelitis with hindlimb paralysis and progressive destruction of the CNS (Fleming et al., 1987; Haring and Perlman, 2001; Lane et al., 1998; Stohlman et al., 2002). Two of the MHV injected animals died during the first week post injection; there is an 80–90% survival rate of animals injected with this viral strain, and the animals usually die during the first 12 days of acute infection. If the animals survive the acute stage of disease there is >95% chance of survival. Control (sham) animals ($n = 8$) were injected with 30 μl of sterile saline alone and did not develop any behavioral or histological deficits.

Transplantation

Twelve days after MHV intracerebral injection, each animal ($n = 7$) received a single injection of 240,000 cells in 2 μl of calcium- and magnesium-free DMEM (Gibco-Invitrogen) at T8 of the spinal cord, using the protocol described in Blakemore and Crang (1992). Briefly, animals were anesthetized with Avertin and received a laminectomy at T8. The spinal process cranial to the laminectomy was immobilized using a micromanipulator and the transplant needle, a 10-μl Hamilton syringe (Hamilton Company, Reno, NV) with a silicon-coated pulled glass tip, was lowered into the spinal cord using a stereotactic manipulator arm. Cell suspensions were injected into one site at the midline of the spinal cord. The needle was removed from the cord 5 min after injection of the cells was complete. In addition, six control animals that received an MHV intracerebral injection received no transplant. One animal died during transplantation/anesthesia. Animals were randomly selected for inclusion in either group and all received an incision to the skin overlying T8 to allow blinded analyses for the duration of the experiment.

Behavioral testing

Behavioral testing of all animals was conducted by a blinded observer, every other day using the 4-point clinical scoring scale (Houtman and Fleming, 1996) where 0 = normal, 1 = limp tail, 2 = waddling gait and partial hindlimb weakness, 3 = complete hindlimb paralysis, 4 = death animal. This 4-point scale was supplemented with a single increment between each point, such that 1.5 = limp tail and partial waddling gait and no hindlimb weakness, 2.5 = hindlimb weakness and partial hindlimb paralysis, 3.5 = complete hindlimb paralysis and moribund disposition. Animals were acclimated and behaviorally tested 1 day before MHV injection. After MHV injection, animals were tested every day. After transplantation, animals were tested every other day for 2 weeks and then every 3rd day until the end of the experiment. Statistical significance was determined using the Mann–Whitney U test.

Histology

Animals were euthanized under chloral hydrate anesthesia (Fisher Scientific) 21 days following transplantation or 33 days after MHV infection and fixed by cardiac perfusion with 4% paraformaldehyde (Fisher Scientific) in 0.1 M PBS, pH 7.4. The length of spinal cord extending 12 mm cranial and 10 mm caudal to the site of implantation was cut

into 1-mm transverse blocks and processed so as to preserve the craniocaudal sequence and orientation. Alternating tissue blocks were processed for resin and cryostat sectioning and analyzed in a blinded fashion. Resin sections were used to determine the area of the ventral and lateral columns, and the number of demyelinated, remyelinated, and normally myelinated axons. Cryostat sections were used to determine spread of BrdU-prelabeled transplanted cells and their differentiation profile.

For resin sectioning, odd numbered blocks were post fixed in 4% glutaraldehyde (Fisher Scientific), then exposed to 1% OsO_4 (Electron Microscopy Sciences, Fort Washington, PA), dehydrated in ascending alcohols, and embedded in Spurr resin (Electron Microscopy Sciences) according to standard protocols. Transverse semi-thin (1 μm) sections were cut from the cranial face of each block, stained with alkaline toluidine blue, cover slipped, and examined by light microscopy on an Olympus AX-80 microscope using OLYMPUS MicroSuite B3SV software. Total areas of the ventral and lateral columns were measured with the 4× objective and averaged. A *t* test was performed to compare the areas of the ventral and lateral columns in transplanted and non-transplanted animals. The state of myelination was determined by assessing the thickness of the myelin sheath in relation to the axon diameter (Guy et al., 1989; Hildebrand and Hahn, 1978). Demyelinated, remyelinated, and normally myelinated axons were counted within 4 × 3750 μm^2 areas, totaling 15 000 μm^2, on each tissue section using the 100× objective with 2× optical zoom. 15 000 μm^2 represents approximately 10% of the total area of remyelination within transplanted animals, which was determined by measuring the total area of remyelination in tissue sections from each block in each animal using the 40× objective, and averaging areas from all animals in each group. These quantitative assessments were conducted throughout the region extending 8 mm cranial and 6 mm caudal to the implantation site. The number of demyelinated axons, remyelinated axons, the total number of axons (normally myelinated plus demyelinated plus remyelinated axons), and the percentage of remyelinated axons (number remyelinated/number total axons) were determined for each of the four regions on each tissue block, averaged, then averaged across animals within each group for each tissue block. A *t* test was performed to compare these values for transplanted and non-transplanted groups. To determine whether the number of remyelinated axons in each animal correlated with the total number of axons in each counting area, remyelinated and total axons counts were each averaged among all four counting areas for all blocks for each animal, and the correlation coefficient between these two values was determined for both transplanted and non-transplanted groups. Statistical analyses were conducted using SPSS software.

For cryostat sectioning, even numbered blocks were cryoprotected in 30% sucrose solution in PBS, embedded in OCT (Fisher Scientific) and frozen sectioned in the transverse plane at 20 μm on a JUNG CM3000 Leica cryostat for anti-BrdU staining. For BrdU staining, sections were washed in PBS, exposed to 50% formamide (Sigma-Aldrich) and 2N hydrochloric acid (Fisher Scientific) for 30 min at 37°C for DNA denaturation, followed by a 30-min exposure to 0.3% H_2O_2 in PBS, then incubated overnight at room temperature with rat anti-BrdU polyclonal antibody (Accurate Chemical and Scientific Corporation) at a 1:200 dilution in 4% NGS. Secondary antibody was biotinylated goat anti-rat heavy and light chain IgG (Sigma-Aldrich). Vectastain ABC (Vector Laboratories) and 3,3′-diaminobenzidine (Vector Laboratories) were used for signal visualization. The number of BrdU-positive cells was counted on three sections 80-μm apart from each tissue block for each animal using OLYMPUS MicroSuite B3SV software, and averaged. The numbers of BrdU-positive cells within corresponding blocks from animals within a group were then averaged. For BrdU, APC-CC1 double staining, sections were washed in PBS, exposed to 2N hydrochloric acid (Fisher Scientific) for 30 min at 37°C for DNA denaturation, and primary antibodies (rat anti-BrdU, 1:200, Accurate Chemical and Scientific Corporation; mouse anti-APC-CC1, 1:20, Oncogene Research Products, San Diego, CA) were diluted in 2% bovine serum albumin and applied to slides overnight at room temperature. Slides were rinsed three times with PBS, incubated for 30 min in 2% bovine serum albumin, and secondary antibodies (Alexa 488 or 594, goat anti-rat or goat anti-mouse IgG H+L, 1:200 dilution in 2% bovine serum albumin; Vector Laboratories) were applied and incubated for 1 h at room temperature.

Results

In vitro differentiation of striatal cultures

Trypan blue analysis indicated that approximately 1.1–1.2 × 10^6 viable cells were obtained from each postnatal day 1 mouse. Floating cell clusters reached approximately 200 μm in diameter after 6 days of culture (Fig. 1a). On day 6, clusters were either (1) dissociated and transplanted into animals or (2) transferred to an adherent substrate in the absence of growth factors, grown for an additional 7 days and assayed for differentiation potential.

As early as 6 h after transfer of cell clusters to an adherent substrate and concomitant growth factor withdrawal, cells started to spread out from the adherent clusters and by 1 day, displayed complex cellular morphologies (Fig. 1b). After 7 days of growth on adherent substrate, oligodendrocytes and astrocytes could be identified by their morphology and immunolabeling. Oligodendrocytes displayed a multipolar morphology with membranous extensions and GalC immunoreactivity (Fig. 1c), whereas astrocytes displayed a flat or stellate morphology and GFAP immunoreactivity (Fig. 1d). Few NeuN immunoreactive neurons (Fig.

1e) and CD11b immunoreactive microglia (results not shown) were detected. No-primary antibody control staining chambers had no positive staining. Different cell types often occupied discrete regions of the culture dishes. A total of 1940 Hoechst-positive cells were counted for the following analyses. Quantification of immunolabeled cells indicated that 85 ± 10.7% (range = 64–96, median = 80) of the total cell population was BrdU immunoreactive following an overnight pulse (Fig. 1f), and that the differentiation protocol yielded 67.4 ± 4.4% oligodendrocytes (range = 60–72, median = 66), 26 ± 7.4% astrocytes (range = 20–40, median = 30) and 6.6 ± 6.2% other cell types (range = 1–13, median = 7), which included NeuN + neurons, CD11b + microglia, and other Hoechst-positive cells not identified by the immunostains tested (Fig. 1g). No difference was observed in the viability or differentiation of BrdU-labeled or -unlabeled cells.

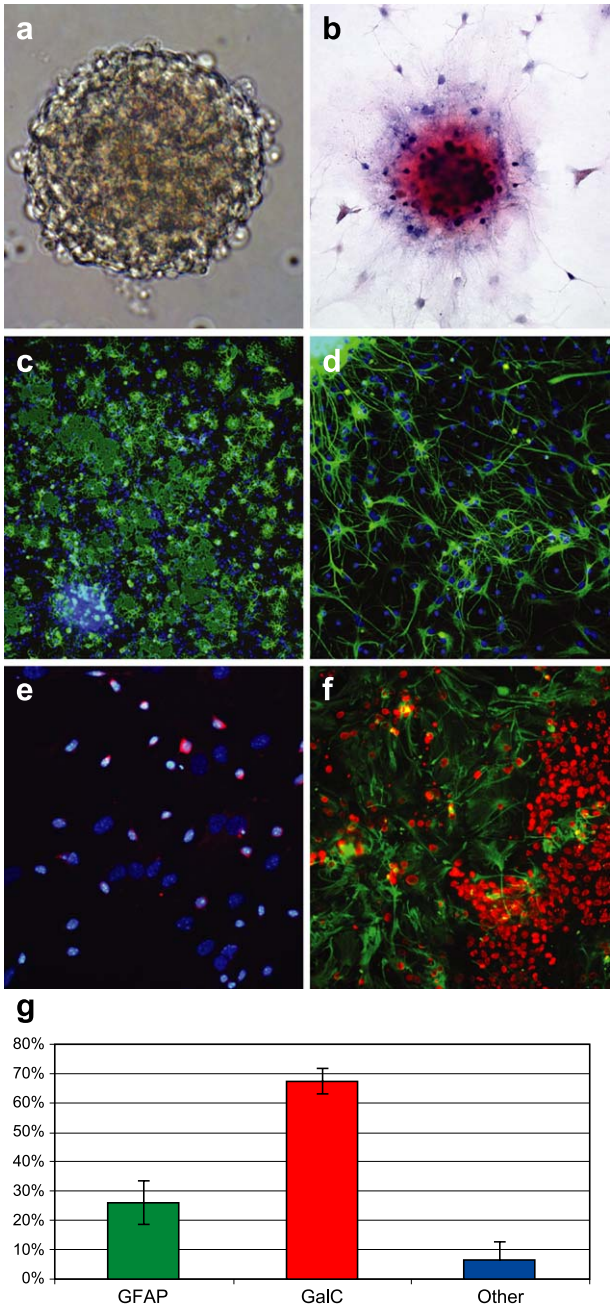

Fig. 1. The differentiation potential of striatal neural precursors can be restricted by culture conditions. (a) Cell cluster after 5 days of growth in non-adherent growth factor containing media, viewed in phase contrast. Cells were grown as free-floating clusters, reaching approximately 200 μm in diameter. (b) Hematoxylin–eosin-stained cell cluster 1 day after transfer to an adherent substrate. Cells spread out from clusters within 6 h of plating, and by 1 day, possess complex morphologies. (c) Multipolar GalC-positive (green) oligodendrocytes were abundant after 7 days of growth on adherent substrate in the absence of growth factors (Hoechst-positive nuclei are blue). (d) GFAP-positive (green) astrocytes were also abundant after 7 days of growth on adherent substrate in the absence of growth factors (Hoechst-positive nuclei are blue). (e) Few NeuN-positive (red) neurons were present (Hoechst-positive nuclei are blue). (f) The majority of cells (85 ± 10.7%) within cultures were BrdU-positive. This field illustrates BrdU-positive (red) GFAP-positive (green) astrocytes. (g) Quantification of cell types after 7 days of growth on adherent substrate in the absence of growth factors indicated that the differentiation protocol yielded 67.4 ± 4.4% oligodendrocytes, 26 ± 7.4% astrocytes, and 6.6 ± 6.2% other cell types, which included NeuN+ neurons, CD11b + microglia, and other Hoechst-positive cells not identified by the immunostains tested. Error bars represent standard deviation. 40× magnification for a and b, 100× for magnification for c and d, 400× magnification for e, 200× magnification for f.

Histological outcome of glial-committed progenitor transplantation

Transplanted glial-committed progenitors, labeled with BrdU before implantation, survived and colonized long lengths of the spinal cord during the 21-day survival period (Fig. 2), and differentiated into mature oligodendrocytes (Fig. 3). BrdU-labeled cells were detected 12 mm cranial and 10 mm caudal to the site of implantation (the extent of tissue examined), and extended throughout the transverse plane of the spinal cord, primarily within white matter tracts. The number of BrdU-labeled cells was greatest around the site of implantation, and fell off sharply 4–6 mm either side of the site of implantation. BrdU-labeled cells were absent in non-transplanted animals (Fig. 2c) and in no-primary antibody control stains of transplanted animals.

Non-transplanted animals infected with MHV develop a demyelinating disease accompanied by mononuclear cell infiltration, widespread myelin destruction, and progressive degeneration of the CNS in the survivors (Fleming et al., 1987; Haring and Perlman, 2001; Liu et al., 2001; Stohlman et al., 2002). Systematic random analyses (Fig. 4a) indicated that numerous demyelinated axons were present (Figs. 4b, e, g) among vacuoles, myelin debris, activated macrophages, lymphocytes, and necrotic cells throughout the region of spinal cord examined, indicative of ongoing pathogenesis. The number of demyelinated axons was not significantly different ($P > 0.05$) in transplanted and non-transplanted animals (Fig. 5a), likely because MHV is an ongoing demyelinating disease generating a similar number of newly demyelinated axons in both non-transplanted and transplanted animals. The number (Fig. 5b) and percentage

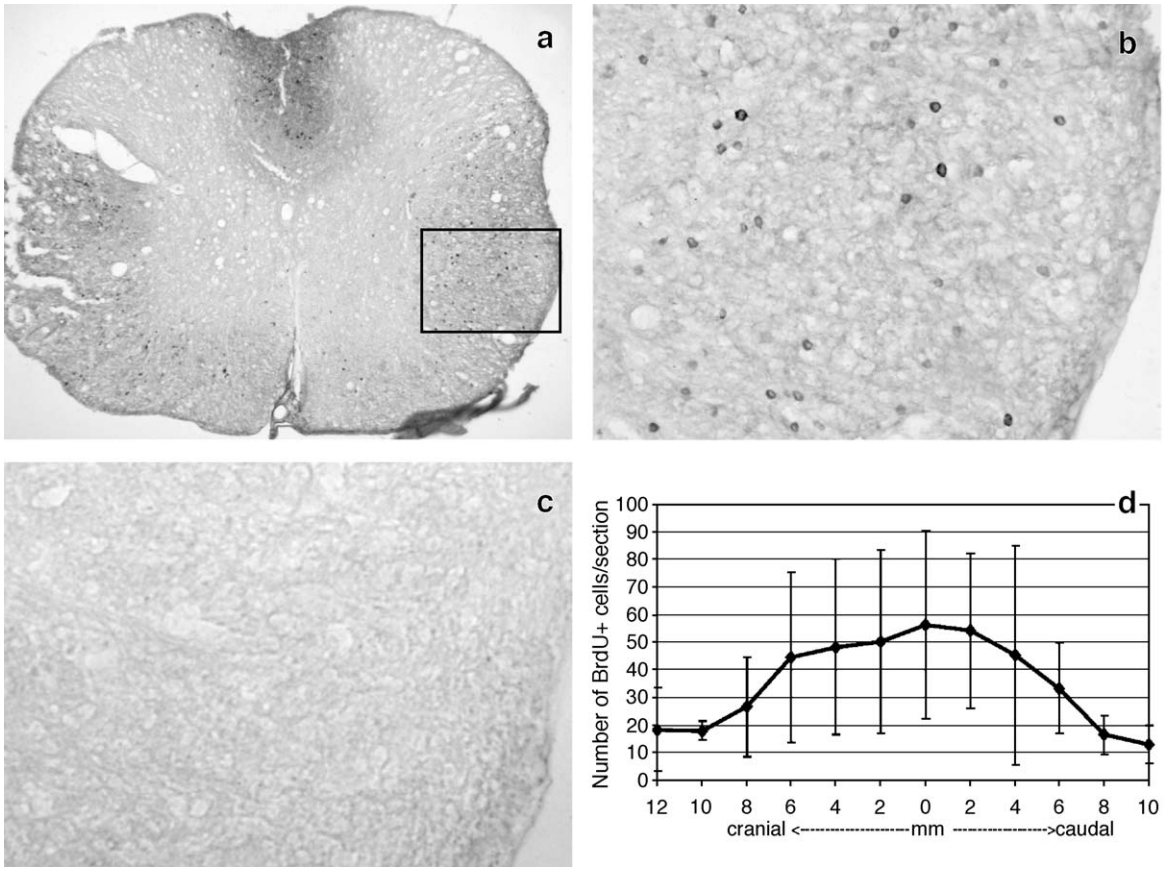

Fig. 2. Transplanted glial-committed progenitor cells survived and migrated during the 21-day survival period. (a): BrdU-stained transverse section of the spinal cord from a MHV-infected mouse 21 days following cell transplantation, 4 mm cranial to the site of implantation. BrdU-positive cells are abundant within the white matter tracts. Box is magnified in b. (b) BrdU-positive cells are evenly distributed within the lateral white matter tracts. (c) BrdU-stained transverse section of the spinal cord from a non-transplanted, MHV injected mouse 33 days following MHV injection. Note the absence of BrdU-labeled cells. (d) Distribution of BrdU-positive cells cranial and caudal to the site of implantation. Error bars represent standard deviation. 100× magnification for a, 400× magnification for b and c.

(Fig. 5c) of remyelinated axons in non-transplanted animals was significantly lower ($P < 0.01$) than in transplanted animals, and composed less than 10% of the total number of axons counted (Fig. 5c). Normally myelinated axons were exceedingly rare at this time point. Control animals injected with saline only did not develop clinical or histopathological deficit.

Transplantation of glial-committed progenitors resulted in widespread remyelination (Figs. 4 and 5). Remyelinated axons were identified by their characteristically thin my-

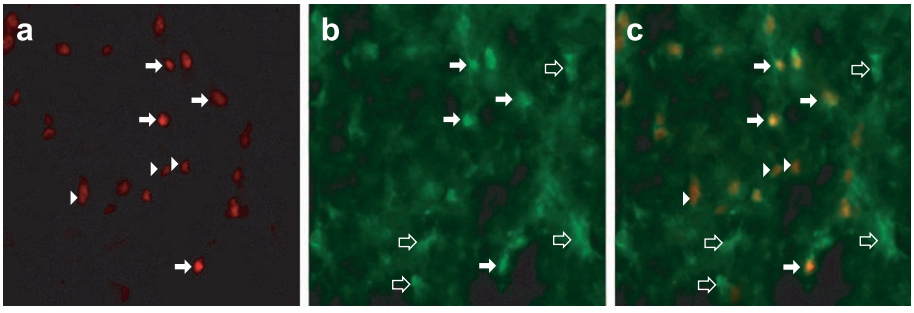

Fig. 3. Transplanted glial-committed progenitor cells differentiated into oligodendrocytes during the 21-day survival period. Double immunohistochemical stains for BrdU to identify transplanted cells and APC-CC1 to identify mature oligodendrocytes. (a) BrdU-stained transverse section of the spinal cord from a MHV-infected mouse 21 days following cell transplantation, 1 mm caudal to the site of implantation. (b) APC-CC1 immunostaining of the same section shown in a. (c) Overlay of a and b. Arrows indicate double-labeled BrdU and APC-CC1 cells, illustrating that transplanted cells differentiated into mature oligodendrocytes. Arrowheads indicate BrdU+ CC1− cells, illustrating transplanted cells that differentiated into other cell types. Arrow profiles indicate BrdU−, CC1+ cells, illustrating endogenous oligodendrocytes. 600× magnification.

elin sheaths (Figs. 4c, f, h) and appeared in aggregates distributed throughout the dorsal, ventral, and lateral columns among demyelinated axons. Remyelination extended 12 mm cranial and 10 mm caudal to the implantation site in six of seven transplanted animals. Counts of remyelinated axons throughout the region extending 8 mm cranial and 6 mm caudal to the implantation site (the extent of our quantification; Fig. 5b) indicated that regions of remyelination contained 54% to 67% remyelinated axons (Fig. 5c). Normally myelinated axons were exceedingly rare at this time point; note that for each tissue block, the number of remyelinated axons (Fig. 5b) plus the number of demyelinated axons (Fig. 5a) approximates the total number of axons (Fig. 5d). One transplanted animal contained few remyelinated axons, similar to non-transplanted animals ($P > 0.1$); immunohistological analysis of this animal revealed that it contained no BrdU-positive cells. We did not observe tumor, teratoma, or non-neuronal tissue formation in transplant recipients, nor did we observe a qualitative difference in Schwann cell presence or remyelination between transplanted and non-transplanted animals.

Counts of the total number of axons (normally myelinated, demyelinated, and remyelinated) within the region extending 8 mm cranial and 6 mm caudal to the transplantation site (the extent of spinal cord examined) suggest that transplanted animals had significantly more axons ($P < 0.01$) within the ventral and lateral columns as compared to non-transplanted animals (Figs. 4g, h and 5d). Area measurements of the ventral and lateral columns revealed no significant difference between animals within and between the transplanted and non-transplanted groups ($P > 0.05$, t test), however, a two-sample t test power analysis indicated that an experimental n of 6 per group was insufficient to conclude statistical significance of the differences between the groups. Nonetheless, these data suggest that the higher number of total axons within transplanted animals was not a result of tissue shrinkage in the transplanted animals.

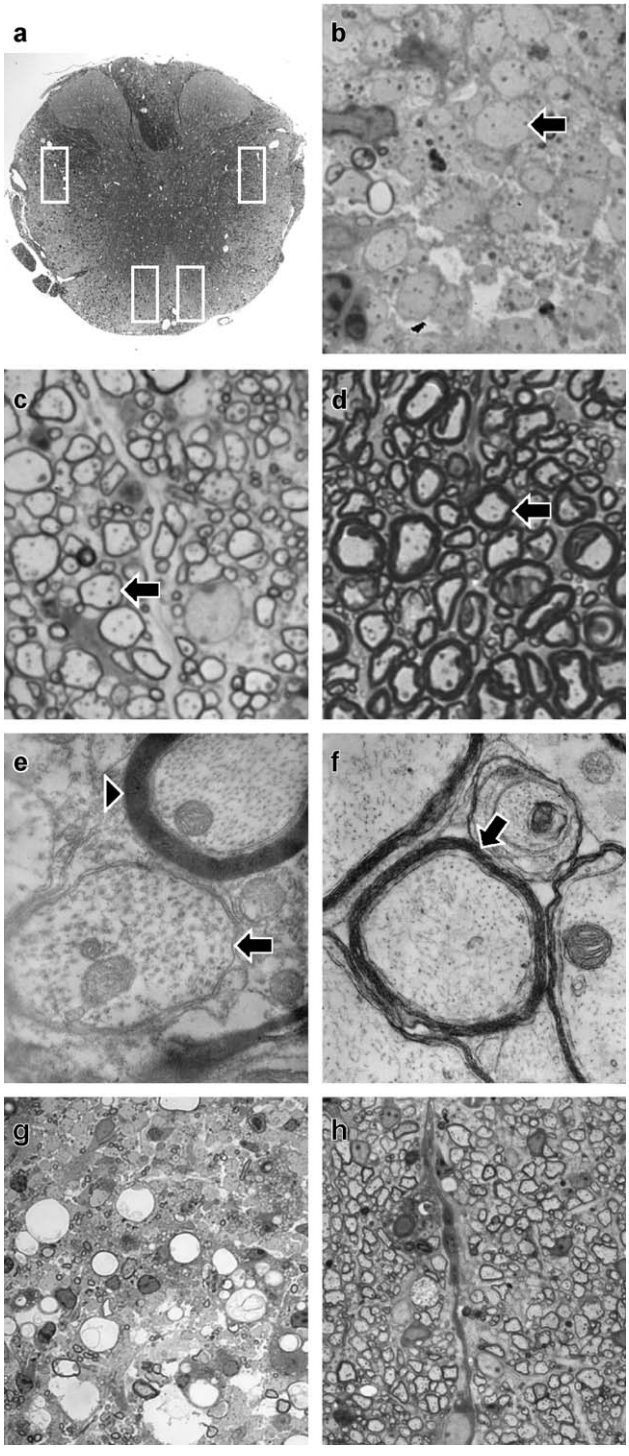

Fig. 4. Transplantation of glial-committed progenitor cells resulted in remyelination. (a) Toluidine blue-stained transverse section of a spinal cord from a transplanted animal showing the areas from which photographs and counts were taken. (b) Toluidine blue-stained transverse section of spinal cord white matter from an MHV-infected mouse 33 days after induction of disease illustrating the predominance of demyelinated axons (arrow). (c) Toluidine blue-stained transverse section of spinal cord white matter from an MHV-infected mouse 33 days after induction of disease and 21 days after transplantation of glial-committed progenitor cells. Note that the vast majority of axons bear thin myelin sheaths (arrow) characteristic of remyelination. (d) Toluidine blue-stained transverse section of spinal cord white matter from a normal mouse, indicating normal myelin sheath thickness (arrow), for comparison with panel c. (e) Electron photomicrograph of spinal cord white matter from an MHV-infected mouse 33 days after induction of disease illustrating a demyelinated axon (arrow) and a normally myelinated axon (arrowhead). (f) Electron photomicrograph of spinal cord white matter from an MHV-infected mouse 33 days after induction of disease and 21 days after transplantation of glial-committed progenitor cells. Note the thin myelin sheaths (arrow) characteristic of remyelination (for comparison, note the thickness of the normal myelin sheath in e (arrowhead). (g) Toluidine blue-stained transverse section of spinal cord white matter from an MHV-infected mouse 33 days after induction of disease illustrating the predominance of demyelinated axons amongst vacuoles, macrophages, lymphocytes, and an enlarged extracellular space. (h) Toluidine blue-stained transverse section of spinal cord white matter from an MHV-infected mouse 33 days after induction of disease and 21 days after transplantation of glial-committed progenitor cells. Note the higher proportion of remyelinated axons and total axon density as compared to non-transplanted animals (g). 40× magnification for a, 2000X for b–d, 39 000 for e and f, 800× magnification for g and h.

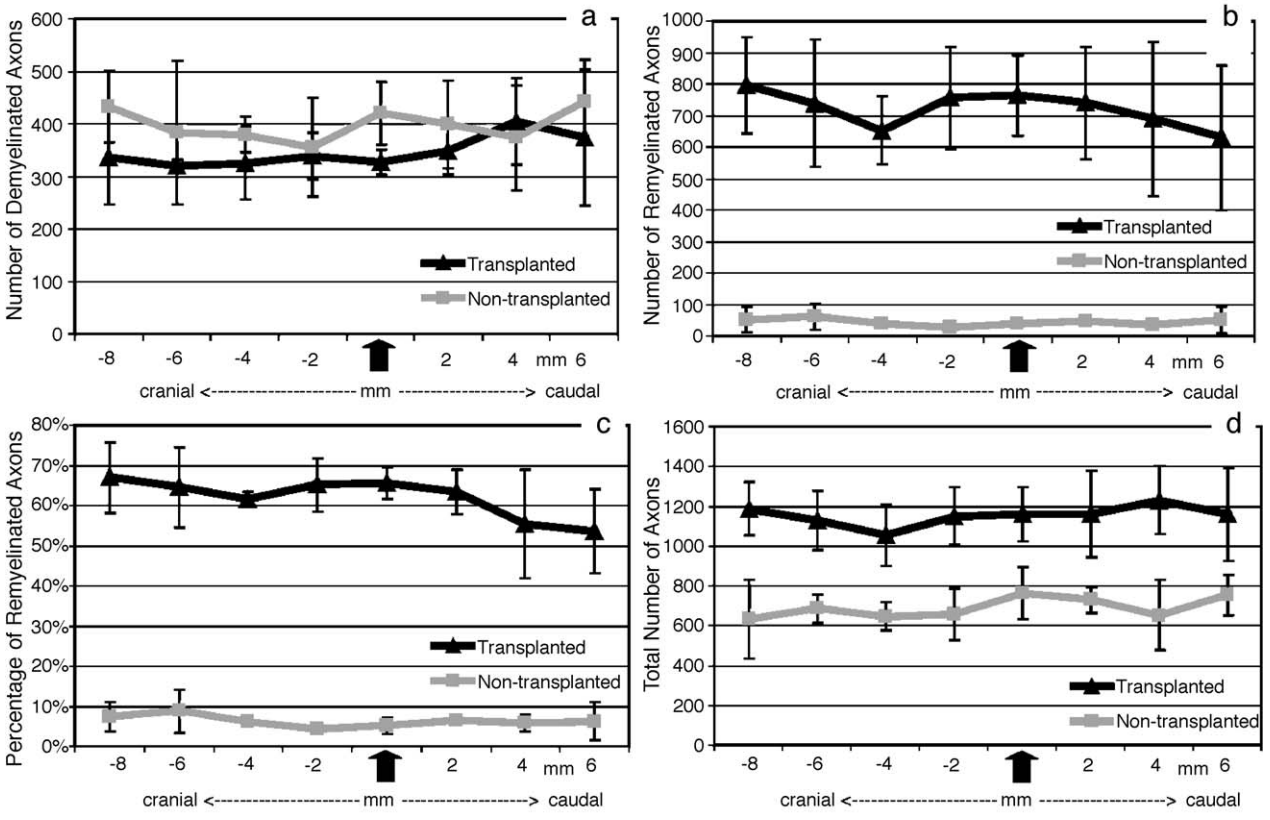

Fig. 5. Transplantation of glial-committed progenitor cells resulted in remyelination and axonal sparing. (a) Demyelinated axons were present in transplanted and non-transplanted animals; their numbers within 15 000 μm^2 of white matter were not statistically different ($P > 0.05$). (b) Remyelination extended 8 mm cranial and 6 mm caudal to the implantation site (arrow) in transplanted animals (the extent of tissue examined) and was significantly greater than the degree of remyelination in non-transplanted animals at every point examined ($P < 0.01$). (c) Throughout this region, 54% to 67% of the total number of axons in the ventral and lateral columns of transplanted animals were remyelinated. Remyelination in non-transplanted animals was significantly less at every point examined ($P < 0.01$). (d) The total number of axons within 15 000 μm^2 of white matter in transplanted animals was approximately 2× the total number of axons within similar regions in non-transplanted animals ($P < 0.01$ for all points), suggesting that remyelination is associated with axonal sparing. Error bars represent standard deviation.

Comparison of the total number of axons with the number of remyelinated axons for each animal within the transplanted group indicated a statistically significant correlation between these two values ($r = 0.953$; $P < 0.05$), indicating that a greater degree of axonal sparing correlated with a greater degree of remyelination.

Behavioral outcome of glial-committed progenitor transplantation

All transplanted animals survived for the duration of the experiment. Non-transplanted animals developed clinical disease typically characterized by a waddling gait and partial hindlimb weakness by 8–9 days post-infection, which progressed to complete hindlimb paralysis by 10 days post-infection, persisting for the duration of the experiment (Fig. 6). Control saline-injected animals displayed normal locomotor behavior throughout the duration of the experiment (all animals scored 0).

Transplantation of glial-committed progenitors resulted in a significant improvement in locomotor abilities (Fig. 6).

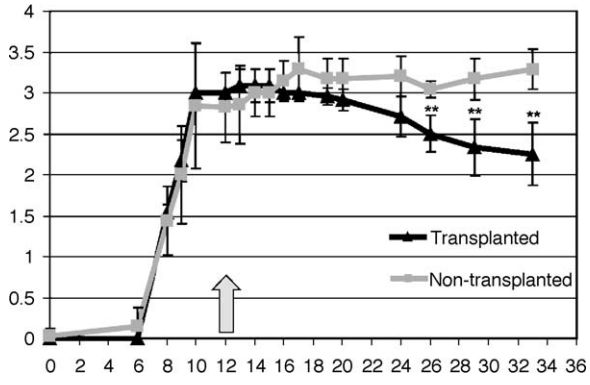

Fig. 6. Transplantation of glial-committed progenitor cells resulted in an improvement in locomotor abilities. Transplanted animals demonstrated a significant improvement ($P < 0.01$) in locomotor abilities beginning 14 days after transplantation (arrow). From 24 days after induction of disease, transplanted animals walked with a waddling gait and partial hindlimb weakness, whereas non-transplanted animals demonstrated complete hindlimb paralysis. Error bars represent standard deviation.

All transplanted animals had complete hindlimb paralysis at the time of transplantation. Six of seven transplanted animals demonstrated a significant ($P < 0.01$) improvement in locomotor abilities beginning 14 days after transplantation, which progressed to weight-supported waddling locomotion with partial hindlimb weakness. One transplanted animal demonstrated no improvement in locomotor abilities; postmortem analysis of this animal revealed that it contained no BrdU-positive transplanted cells and a degree of remyelination that was not significantly different ($P > 0.1$) from non-transplanted animals.

Discussion

Cell replacement strategies must contend with the fact that the differentiation of transplanted cells is strongly influenced by the environmental signals and cellular deficiencies operating at the site of implantation. For example, stem cells isolated from the adult hippocampus generate new hippocampal neurons and glia following transplantation into the hippocampi of other animals, while these same cells generate olfactory bulb neurons expressing appropriate neurotransmitter phenotypes following transplantation into the rostral migratory stream, or glial cells following transplantation into regions of the CNS which do not normally generate neurons in the adult (Gage et al., 1995; Suhonen et al., 1996). These influences present formidable challenges to cell replacement strategies aimed at promoting repair of neurodegenerative disease or injury due to the complex and reactive environment of such lesions, and point towards lineage commitment of multipotent cells before transplantation (Keirstead, 2001).

Our differentiation protocol resulted in the generation of oligodendrocytes and astrocytes in high yield (67.4% and 26%, respectively) from postnatal day 1 derived striatal neural precursors (Fig. 1), supporting previous studies using a similar differentiation protocol (Ben-Hur et al., 1998). Cellular migration in vitro was evident as early as 6 h, and cellular differentiation in vitro was evident as early as 1 day, after transfer of cell clusters to an adherent substrate and concomitant growth factor withdrawal.

To assess migration and differentiation in vivo, undifferentiated prelabeled glial-committed progenitors were transplanted into regions of demyelination in the MHV model of MS. Intracerebral injection of the J2.2v-1 strain of MHV results in initial viral replication in the ependymal cells lining the ventricles, which subsequently extends to the central canal, gray and white matter of the spinal cord. Infectious virus is usually eliminated by days 12–14 post infection, but is not completely cleared. Acute encephalomyelitis with myelin loss is present by day 5 and extends rapidly in the anterior funiculi. An immune-mediated demyelinating encephalomyelitis with hindlimb paralysis and progressive destruction of the CNS then follows; although some remyelination takes place, the initiation of new foci of demyelination likely continues for the entire life of the mouse (Fleming et al., 1987; Haring and Perlman, 2001; Lane et al., 1998; Liu et al., 2001; Stohlman and Hinton, 2001; Stohlman et al., 2002). In the current study, undifferentiated glial-committed progenitors were transplanted into the thoracic spinal cords of mice with fulminate demyelinating pathology and complete hindlimb paralysis as a result of MHV infection. Transplanted cells survived for the duration of the 21-day post-transplantation period and spread throughout the mediolateral extent of the spinal cord as well as 12 mm cranial and 10 mm caudal to the site of implantation, the extent of the tissue being examined (Fig. 2). These findings demonstrate that transplanted progenitor cells are capable of extensive migration throughout regions of ongoing pathogenesis. Survival and extensive migration of transplanted gliogenic cell populations has been demonstrated in the developing normal CNS (Jacque et al., 1992), myelin-deficient mutant CNS (Brustle et al., 1999; Gansmuller et al., 1991; Liu et al., 2000; Tontsch et al., 1994), chemically demyelinated CNS (Groves et al., 1993; Keirstead and Blakemore, 1999), and in inflamed white matter tracts in the EAE model of MS (Ben-Hur et al., 2003; Pluchino et al., 2003). However, the ability of gliogenic cell populations to survive and migrate in these environments does not indicate that they will do so in the intact normal adult CNS. When glial progenitors (Franklin et al., 1996; O'Leary and Blakemore, 1997) are transplanted into the intact normal adult CNS, they fail to survive or migrate; only when the cells are placed in the immediate vicinity of active regions of demyelination, where survival factors are elevated (Hinks and Franklin, 1999), do they enter the lesion. These findings suggest that the survival and extensive migration of cells in our study was due in part to the continuity of pathology throughout the region of migration.

Transplantation of glial-committed progenitors resulted in extensive remyelination, ranging from 54% to 67% of the axons present within randomly selected regions of the spinal cord (Figs. 4 and 5). The in vitro (Fig. 1) and in vivo (Fig. 3) differentiation profile of these cells, the presence of extensive remyelination only in transplanted animals (Figs. 5b, c), and the presence of remyelination throughout the region over which transplanted cells migrated (Figs. 2d and 5b) suggest that remyelination was conducted by the transplanted cell population. Nonetheless, we cannot rule out the possibility that remyelination in transplanted animals was carried out by endogenous cells that may have been activated as a result of trophic support by the transplanted population.

Cumulative axonal loss has recently been demonstrated in several human (Bitsch et al., 2000; Ferguson et al., 1997; Trapp et al., 1998) and rodent (Bjartmar et al., 1999; Griffiths et al., 1998; Yin et al., 1998) demyelinating pathologies, using in vivo magnetic resonance imaging (Stevenson and Miller, 1999; Van Waesberghe et al., 1999), in vivo magnetic resonance spectroscopy (Arnold

et al., 1994; Matthews et al., 1998), morphological analysis of brain sections (Ferguson et al., 1997; Trapp et al., 1998), and biochemical methods (Bjartmar et al., 2000). Chronic demyelination is a probable cause of such axonal loss (Bjartmar and Trapp, 2001). To determine whether remyelination was associated with axonal sparing in the current study, total axon numbers were determined within the ventral and lateral columns of transplanted and non-transplanted animal groups 33 days after induction of disease. Although the area of the ventral and lateral columns were not significantly different between the transplanted and non-transplanted groups ($P > 0.05$, t test), the total number of axons within the ventral and lateral columns of transplanted remyelinated animals was approximately 2× the number of axons within the ventral and lateral columns of non-transplanted animals (Fig. 5d). Furthermore, comparison of the total number of axons with the number of remyelinated axons for each animal within the transplanted group indicated a statistically significant correlation between these two values ($r = 0.953$). These findings suggest that a greater degree of axonal sparing correlated with a greater degree of remyelination. Reduced axonal loss has also been shown after intravenous or intrathecal neurosphere transplantation in the EAE mouse model of MS (Pluchino et al., 2003). These data support the view that chronic demyelination is a cause of axonal loss, and suggest that transplant-mediated remyelination protects axons from degeneration/transection. Further studies are required to determine the molecular mechanisms underlying demyelination-associated axonal degeneration/transection.

Transplantation of glial-committed progenitors resulted in a significant improvement in locomotor abilities beginning 14 days after transplantation, which progressed to weight-supported waddling locomotion with partial hindlimb weakness (Fig. 6). Non-transplanted animals remained completely paralyzed throughout this time period (Fig. 6). In regions of experimental demyelination induced by lysolecithin (Smith et al., 1979, 1981; Yezierski et al., 1992) or ethidium bromide (Felts and Smith, 1992), return of secure axonal conduction occurs at the same time as spontaneous remyelination and transplanted glial cells have been shown to improve conduction velocity to near-normal values in myelin-deficient rats (Utzschneider et al., 1994) and ethidium bromide lesions (Honmou et al., 1996). Transplantation of clonal neural cells into the intracerebroventricular system of the shiverer mice at birth resulted in myelination of up to 52% of host neuronal processes and reduced the symptomatic tremor in some animals (Yandava et al., 1999). Thus, it is intriguing that the time course of behavioral improvement following transplantation in the current study approximates the time required for remyelination (Pender et al., 1989; Smith et al., 1981).

Our findings demonstrate that transplant-mediated remyelination is possible in the complex and reactive environment of the MHV model of multiple sclerosis. Transplant-mediated remyelination has been demonstrated in regions of the CNS subjected to experimental demyelination or in myelin mutants, environments that are characterized by a clear cellular deficit, a largely non-reactive CNS environment, and a lack of inflammation. Thus, transplantation of embryonic stem cell-derived precursors (Brustle et al., 1999) or oligodendrocyte progenitors (Zhang et al., 1999) into postnatal myelin-deficient rats resulted in differentiation of transplanted cells into myelinating oligodendrocytes and astrocytes. Multipotential PSA-NCAM + neural precursors isolated from the postnatal rat brain have been shown to differentiate into oligodendrocytes, Schwann cells, and astrocytes following transplantation, to completely remyelinate regions of acute demyelination in the adult rat induced by ethidium bromide injection into x-irradiated dorsal column white matter (Keirstead et al., 1999). Similarly, transplantation of embryonic stem cells into regions of ethidium bromide induced demyelination in the adult rat spinal cord or into myelin-deficient shiverer mutant mice, resulted in the generation of stem cell-derived oligodendrocytes that were capable of myelinating axons (Liu et al., 2000). More recently, transplant-mediated remyelination has been illustrated in the EAE model of MS, following intravenous or intrathecal injection of adult neural precursor cells (Pluchino et al., 2003). Our findings confirm and extend those outlined above, in demonstrating that intraspinal transplant-mediated remyelination can occur in the fulminate neurodegenerative environment of the MHV model of MS and is associated with locomotor improvement.

The ability of glial cell preparations to remyelinate in such models does not necessarily indicate that their transplantation into demyelinated lesions in clinical disease will be successful (Stangel, 2002). Firstly, transplanted cells may be subject to the same demyelinating process that led to the development of the initial pathology. Notably, the viral 'trigger' of pathology in the MHV model of MS is largely cleared by 12 days post-infection (Lane et al., 1998; Stohlman and Hinton, 2001), before the time of implantation in the current study. Secondly, the inability of glial progenitors to migrate through normal tissue (O'Leary and Blakemore, 1997) renders them less than ideal for remyelinating disparate foci of demyelination as seen in clinical disease (Prineas et al., 1993a). Thirdly, human transplantation necessitates a human progenitor or stem cell population that is capable of amplification and is myelinogenic. Although robust amplification of human embryonic stem cells has been achieved (Carpenter et al., 2001; Reubinoff et al., 2001), the conditions needed to differentiate them into a remyelination-competent transplant population have not yet been defined. And fourthly, the gliotic environment of clinical lesions, which may contribute to the failure of endogenous remyelination, may prohibit the transplant population from effecting repair. Clearly, several key issues must be addressed before a cellular replacement strategy can be considered for the treatment of human demyelinating pathologies such as MS.

Acknowledgments

We thank Oswald Steward for discussion and advice. We thank Michael Liu for assistance with viral injections, Rafael Gonzalez and Giovanna Bernal for assistance with animal surgeries, and Josh Kunellis for assistance with tissue processing. This project was supported by the National Multiple Sclerosis Society, and individual donations to the Reeve-Irvine Research Center.

References

Arnold, D.L., Riess, G.T., Matthews, P.M., Francis, G.S., Collins, D.L., Wolfson, C., Antel, J.P., 1994. Use of proton magnetic resonance spectroscopy for monitoring disease progression in multiple sclerosis. Ann. Neurol. 36, 76–82.

Ben-Hur, T., Rogister, B., Murray, K., Rougon, G., Dubois-Dalcq, M., 1998. Growth and fate of PSA-NCAM+ precursors of the postnatal brain. J. Neurosci. 18, 5777–5788.

Ben-Hur, T., Einstein, O., Mizrachi-Kol, R., Ben-Menachem, O., Reinhartz, E., Karussis, D., Abramsky, O., 2003. Transplanted multipotential neural precursor cells migrate into the inflamed white matter in response to experimental autoimmune encephalomyelitis. Glia 41, 73–80.

Bitsch, A., Schuchardt, J., Bunkowski, S., Kuhlmann, T., Bruck, W., 2000. Acute axonal injury in multiple sclerosis. Correlation with demyelination and inflammation. Brain 123, 1174–1183.

Bjartmar, C., Trapp, B.D., 2001. Axonal and neuronal degeneration in multiple sclerosis: mechanisms and functional consequences. Curr. Opin. Neurol. 14, 271–278.

Bjartmar, C., Yin, X., Trapp, B.D., 1999. Axonal pathology in myelin disorders. J. Neurocytol. 28, 383–395.

Bjartmar, C., Kidd, G., Mork, S., Rudick, R., Trapp, B.D., 2000. Neurological disability correlates with spinal cord axonal loss and reduced *N*-acetyl aspartate in chronic multiple sclerosis patients. Ann. Neurol. 48, 893–901.

Blakemore, W.F., 1973. Remyelination of the superior cerebellar peduncle in the mouse following demyelination induced by feeding cuprizone. J. Neurol. Sci. 20, 73–83.

Blakemore, W.F., 1974. Remyelination of the superior cerebellar peduncle in old mice following demyelination induced by cuprizone. J. Neurol. Sci. 22, 121–126.

Blakemore, W.F., 1975. Remyelination by Schwann cells of axons demyelinated by intraspinal injection of 6-aminonicotinamide in the rat. J. Neurocytol. 4, 745–757.

Blakemore, W.F., 1982. Ethidium bromide induced demyelination in the spinal cord of the cat. Neuropathol. Appl. Neurobiol. 8, 365–375.

Blakemore, W.F., Crang, A.J., 1992. Transplantation of Glial Cells into Areas of Demyelination in the Adult Rat Spinal Cord. Oxford UP, Oxford.

Brustle, O., Jones, K.N., Learish, R.D., Karram, K., Choudhary, K., Wiestler, O.D., Duncan, I.D., McKay, R.D., 1999. Embryonic stem cell-derived glial precursors: a source of myelinating transplants. Science 285, 754–756.

Carpenter, M.K., Inokuma, M.S., Denham, J., Mujtaba, T., Chiu, C.P., Rao, M.S., 2001. Enrichment of neurons and neural precursors from human embryonic stem cells. Exp. Neurol. 172, 383–397.

De Stefano, N., Matthews, P.M., Fu, L., Narayanan, S., Stanley, J., Francis, G.S., Antel, J.P., Arnold, D.L., 1998. Axonal damage correlates with disability in patients with relapsing–remitting multiple sclerosis. Results of a longitudinal magnetic resonance spectroscopy study. Brain 121, 1469–1477.

Duncan, I.D., Hammang, J.P., Jackson, K.F., Wood, P.M., Bunge, R.P., Langford, L., 1988. Transplantation of oligodendrocytes and Schwann cells into the spinal cord of the myelin-deficient rat. J. Neurocytol. 17, 351–360.

Felts, P.A., Smith, K.J., 1992. Conduction properties of central nerve fibers remyelinated by Schwann cells. Brain Res. 574, 178–192.

Ferguson, B., Matyszak, M.K., Esiri, M.M., Perry, V.H., 1997. Axonal damage in acute multiple sclerosis lesions. Brain 120, 393–399.

Fleming, J.O., Trousdale, M.D., Bradbury, J., Stohlman, S.A., Weiner, L.P., 1987. Experimental demyelination induced by coronavirus JHM (MHV-4): molecular identification of a viral determinant of paralytic disease. Microb. Pathog. 3, 9–20.

Franklin, R.J., Bayley, S.A., Blakemore, W.F., 1996. Transplanted CG4 cells (an oligodendrocyte progenitor cell line) survive, migrate, and contribute to repair of areas of demyelination in X-irradiated and damaged spinal cord but not in normal spinal cord. Exp. Neurol. 137, 263–276.

Gage, F.H., Coates, P.W., Palmer, T.D., Kuhn, H.G., Fisher, L.J., Suhonen, J.O., Peterson, D.A., Suhr, S.T., Ray, J., 1995. Survival and differentiation of adult neuronal progenitor cells transplanted to the adult brain. Proc. Natl. Acad. Sci. U. S. A. 92, 11879–11883.

Gansmuller, A., Clerin, E., Kruger, F., Gumpel, M., Lachapelle, F., 1991. Tracing transplanted oligodendrocytes during migration and maturation in the shiverer mouse brain. Glia 4, 580–590.

Griffiths, I., Klugmann, M., Anderson, T., Yool, D., Thomson, C., Schwab, M.H., Schneider, A., Zimmermann, F., McCulloch, M., Nadon, N., Nave, K.A., 1998. Axonal swellings and degeneration in mice lacking the major proteolipid of myelin. Science 280, 1610–1613.

Groves, A.K., Barnett, S.C., Franklin, R.J., Crang, A.J., Mayer, M., Blakemore, W.F., Noble, M., 1993. Repair of demyelinated lesions by transplantation of purified O-2A progenitor cells. Nature 362, 453–455.

Gumpel, M., Gout, O., Lubetzki, C., Gansmuller, A., Baumann, N., 1989. Myelination and remyelination in the central nervous system by transplanted oligodendrocytes using the shiverer model. Discussion on the remyelinating cell population in adult mammals. Dev. Neurosci. 11, 132–139.

Guy, J., Ellis, E.A., Kelley, K., Hope, G.M., 1989. Spectra of G ratio, myelin sheath thickness, and axon and fiber diameter in the guinea pig optic nerve. J. Comp. Neurol. 287, 446–454.

Haring, J., Perlman, S., 2001. Mouse hepatitis virus. Curr. Opin. Microbiol. 4, 462–466.

Herndon, R.M., Price, D.L., Weiner, L.P., 1977. Regeneration of oligodendroglia during recovery from demyelinating disease. Science 195, 693–694.

Hildebrand, C., Hahn, R., 1978. Relation between myelin sheath thickness and axon size in spinal cord white matter of some vertebrate species. J. Neurol. Sci. 38, 421–434.

Hinks, G.L., Franklin, R.J., 1999. Distinctive patterns of PDGF-A, FGF-2, IGF-I, and TGF-beta1 gene expression during remyelination of experimentally-induced spinal cord demyelination. Mol. Cell. Neurosci. 14, 153–168.

Honmou, O., Felts, P.A., Waxman, S.G., Kocsis, J.D., 1996. Restoration of normal conduction properties in demyelinated spinal cord axons in the adult rat by transplantation of exogenous Schwann cells. J. Neurosci. 16, 3199–3208.

Houtman, J.J., Fleming, J.O., 1996. Pathogenesis of mouse hepatitis virus-induced demyelination. J. NeuroVirol. 2, 361–376.

Jacque, C., Quinonero, J., Collins, P.V., Villarroya, H., Suard, I., 1992. Comparative migration and development of astroglial and oligodendroglial cell populations from a brain xenograft. J. Neurosci. 12, 3098–3106.

Jeffery, N.D., Blakemore, W.F., 1995. Remyelination of mouse spinal cord axons demyelinated by local injection of lysolecithin. J. Neurocytol. 24, 775–781.

Jeffery, N.D., Blakemore, W.F., 1997. Locomotor deficits induced by experimental spinal cord demyelination are abolished by spontaneous remyelination. Brain 120, 27–37.

Jeffery, N.D., Crang, A.J., O'Leary, M.T., Hodge, S.J., Blakemore, W.F., 1999. Behavioural consequences of oligodendrocyte progenitor cell

transplantation into experimental demyelinating lesions in the rat spinal cord. Eur. J. Neurosci. 11, 1508–1514.
Keirstead, H.S., 2001. Stem cell transplantation into the central nervous system and the control of differentiation. J. Neurosci. Res. 63, 233–236.
Keirstead, H.S., Blakemore, W.F., 1999. The role of oligodendrocytes and oligodendrocyte progenitors in CNS remyelination. Adv. Exp. Med. Biol. 468, 183–197.
Keirstead, H.S., Ben-Hur, T., Rogister, B., O'Leary, M.T., Dubois-Dalcq, M., Blakemore, W.F., 1999. Polysialylated neural cell adhesion molecule-positive CNS precursors generate both oligodendrocytes and Schwann cells to remyelinate the CNS after transplantation. J. Neurosci. 19, 7529–7536.
Lane, T.E., Asensio, V.C., Yu, N., Paoletti, A.D., Campbell, I.L., Buchmeier, M.J., 1998. Dynamic regulation of alpha- and beta-chemokine expression in the central nervous system during mouse hepatitis virus-induced demyelinating disease. J. Immunol. 160, 970–978.
Liu, S., Qu, Y., Stewart, T.J., Howard, M.J., Chakrabortty, S., Holekamp, T.F., McDonald, J.W., 2000. Embryonic stem cells differentiate into oligodendrocytes and myelinate in culture and after spinal cord transplantation. Proc. Natl. Acad. Sci. U. S. A. 97, 6126–6131.
Liu, M.T., Keirstead, H.S., Lane, T.E., 2001. Neutralization of the chemokine CXCL10 reduces inflammatory cell invasion and demyelination and improves neurological function in a viral model of multiple sclerosis. J. Immunol. 167, 4091–4097.
Matthews, P.M., De Stefano, N., Narayanan, S., Francis, G.S., Wolinsky, J.S., Antel, J.P., Arnold, D.L., 1998. Putting magnetic resonance spectroscopy studies in context: axonal damage and disability in multiple sclerosis. Semin. Neurol. 18, 327–336.
Miller, D.J., Rodriguez, M., 1995. Spontaneous and induced remyelination in multiple sclerosis and the Theiler's virus model of central nervous system demyelination. Microsc. Res. Tech. 32, 230–245.
Moore, G.R., Traugott, U., Stone, S.H., Raine, C.S., 1985. Dose-dependency of MBP-induced demyelination in the guinea pig. J. Neurol. Sci. 70, 197–205.
Murray, P.D., McGavern, D.B., Sathornsumetee, S., Rodriguez, M., 2001. Spontaneous remyelination following extensive demyelination is associated with improved neurological function in a viral model of multiple sclerosis. Brain 124, 1403–1416.
O'Leary, M.T., Blakemore, W.F., 1997. Oligodendrocyte precursors survive poorly and do not migrate following transplantation into the normal adult central nervous system. J. Neurosci. Res. 48, 159–167.
Ozawa, K., Suchanek, G., Breitschopf, H., Bruck, W., Budka, H., Jellinger, K., Lassmann, H., 1994. Patterns of oligodendroglia pathology in multiple sclerosis. Brain 117, 1311–1322.
Pender, M.P., Nguyen, K.B., Willenborg, D.O., 1989. Demyelination and early remyelination in experimental allergic encephalomyelitis passively transferred with myelin basic protein-sensitized lymphocytes in the Lewis rat. J. Neuroimmunol. 25, 125–142.
Pluchino, S., Quattrini, A., Brambilla, E., Gritti, A., Salani, G., Dina, G., Galli, R., Del Carro, U., Amadio, S., Bergami, A., Furlan, R., Comi, G., Vescovi, A.L., Martino, G., 2003. Injection of adult neurospheres induces recovery in a chronic model of multiple sclerosis. Nature 422, 688–694.
Prineas, J.W., Barnard, R.O., Kwon, E.E., Sharer, L.R., Cho, E.S., 1993a. Multiple sclerosis: remyelination of nascent lesions. Ann. Neurol. 33, 137–151.
Prineas, J.W., Barnard, R.O., Revesz, T., Kwon, E.E., Sharer, L., Cho, E.S., 1993b. Multiple sclerosis. Pathology of recurrent lesions. Brain 116, 681–693.
Reubinoff, B.E., Pera, M.F., Vajta, G., Trounson, A.O., 2001. Effective cryopreservation of human embryonic stem cells by the open pulled straw vitrification method. Hum. Reprod. 16, 2187–2194.
Rodriguez, M., Lennon, V.A., 1990. Immunoglobulins promote remyelination in the central nervous system. Ann. Neurol. 27, 12–17.
Rodriguez, M., Lennon, V.A., Benveniste, E.N., Merrill, J.E., 1987. Remyelination by oligodendrocytes stimulated by antiserum to spinal cord. J. Neuropathol. Exp. Neurol. 46, 84–95.
Sasaki, M., Ide, C., 1989. Demyelination and remyelination in the dorsal funiculus of the rat spinal cord after heat injury. J. Neurocytol. 18, 225–239.
Shields, S.A., Gilson, J.M., Blakemore, W.F., Franklin, R.J., 1999. Remyelination occurs as extensively but more slowly in old rats compared to young rats following gliotoxin-induced CNS demyelination. Glia 28, 77–83.
Smith, E.J., Blakemore, W.F., McDonald, W.I., 1979. Central remyelination restores secure conduction. Nature 280, 395–396.
Smith, K.J., Blakemore, W.F., McDonald, W.I., 1981. The restoration of conduction by central remyelination. Brain 104, 383–404.
Stangel, M., 2002. Transplantation of myelinating cells as regenerative therapy for multiple sclerosis—Experimental basis and present state of clinical studies. Nervenarzt 73, 937–945.
Stevenson, V.L., Miller, D.H., 1999. Magnetic resonance imaging in the monitoring of disease progression in multiple sclerosis. Mult. Scler. 5, 268–272.
Stohlman, S.A., Hinton, D.R., 2001. Viral induced demyelination. Brain Pathol. 11, 92–106.
Stohlman, S.A., Ramakrishna, C., Tschen, S.I., Hinton, D.R., Bergmann, C.C., 2002. The art of survival during viral persistence. J. NeuroVirol. 8 (Suppl. 2), 53–58.
Suhonen, J.O., Peterson, D.A., Ray, J., Gage, F.H., 1996. Differentiation of adult hippocampus-derived progenitors into olfactory neurons in vivo. Nature 383, 624–627.
Suzuki, K., Andrews, J.M., Waltz, J.M., Terry, R.D., 1969. Ultrastructural studies of multiple sclerosis. Lab. Invest. 20, 444–454.
Tontsch, U., Archer, D.R., Dubois-Dalcq, M., Duncan, I.D., 1994. Transplantation of an oligodendrocyte cell line leading to extensive myelination. Proc. Natl. Acad. Sci. U. S. A. 91, 11616–11620.
Trapp, B.D., Peterson, J., Ransohoff, R.M., Rudick, R., Mork, S., Bo, L., 1998. Axonal transection in the lesions of multiple sclerosis. N. Engl. J. Med. 338, 278–285.
Utzschneider, D.A., Archer, D.R., Kocsis, J.D., Waxman, S.G., Duncan, I.D., 1994. Transplantation of glial cells enhances action potential conduction of amyelinated spinal cord axons in the myelin-deficient rat. Proc. Natl. Acad. Sci. U. S. A. 91, 53–57.
van Waesberghe, J.H., Kamphorst, W., De Groot, C.J., van Walderveen, M.A., Castelijns, J.A., Ravid, R., Lycklama a Nijeholt, G.J., van der Valk, P., Polman, C.H., Thompson, A.J., Barkhof, F., 1999. Axonal loss in multiple sclerosis lesions: magnetic resonance imaging insights into substrates of disability. Ann. Neurol. 46, 747–754.
Yajima, K., Suzuki, K., 1979. Demyelination and remyelination in the rat central nervous system following ethidium bromide injection. Lab. Invest. 41, 385–392.
Yandava, B.D., Billinghurst, L.L., Snyder, E.Y., 1999. "Global" cell replacement is feasible via neural stem cell transplantation: evidence from the dysmyelinated shiverer mouse brain. Proc. Natl. Acad. Sci. U. S. A. 96, 7029–7034.
Yao, D.L., Liu, X., Hudson, L.D., Webster, H.D., 1995. Insulin-like growth factor I treatment reduces demyelination and up-regulates gene expression of myelin-related proteins in experimental autoimmune encephalomyelitis. Proc. Natl. Acad. Sci. U. S. A. 92, 6190–6194.
Yezierski, R.P., Devon, R.M., Vicedomini, J.P., Broton, J.G., 1992. Effects of dorsal column demyelination on evoked potentials in nucleus gracilis. J. Neurotrauma 9, 231–244.
Yin, X., Crawford, T.O., Griffin, J.W., Tu, P., Lee, V.M., Li, C., Roder, J., Trapp, B.D., 1998. Myelin-associated glycoprotein is a myelin signal that modulates the caliber of myelinated axons. J. Neurosci. 18, 1953–1962.
Zhang, S.C., Ge, B., Duncan, I.D., 1999. Adult brain retains the potential to generate oligodendroglial progenitors with extensive myelination capacity. Proc. Natl. Acad. Sci. U. S. A. 96, 4089–4094.